Cell, Vol. 120, 49–58, January 14, 2005, Copyright ©2005 by Elsevier Inc. DOI 10.1016/j.cell.2004.11.042

mRNA Helicase Activity of the Ribosome

Seyedtaghi Takyar,[1] Robyn P. Hickerson, and Harry F. Noller*
Department of Molecular, Cell, and Developmental Biology and Center for Molecular Biology of RNA
University of California, Santa Cruz
Santa Cruz, California 95064

Summary

Most mRNAs contain secondary structure, yet their codons must be in single-stranded form to be translated. Until now, no helicase activity has been identified which could account for the ability of ribosomes to translate through downstream mRNA secondary structure. Using an oligonucleotide displacement assay, together with a stepwise in vitro translation system made up of purified components, we show that ribosomes are able to disrupt downstream helices, including a perfect 27 base pair helix of predicted $T_m = 70°$. Using helices of different lengths and registers, the helicase active site can be localized to the middle of the downstream tunnel, between the head and shoulder of the 30S subunit. Mutation of residues in proteins S3 and S4 that line the entry to the tunnel impairs helicase activity. We conclude that the ribosome itself is an mRNA helicase and that proteins S3 and S4 may play a role in its processivity.

Introduction

Many mRNAs have been shown to have extensive secondary structure within their coding sequences (Favre et al., 1975; Holder and Lingrel, 1975; Min Jou et al., 1972), and even RNA of random sequence has been found to be ~50% base paired (Doty et al., 1959). This poses a potential thermodynamic and kinetic barrier to protein synthesis. Yet, the translation machinery is highly efficient at unwinding helical structure in mRNA during the elongation phase (Lingelbach and Dobberstein, 1988). In some cases, this unwinding capacity plays a part in translational regulation because it appears not to function during translational initiation. For example, the replicase gene of the RNA phage MS2 cannot be read until the upstream coat protein gene is translated because the start codon for the replicase is base paired to an internal segment of the coat protein gene (Min Jou et al., 1972; van Himbergen et al., 1993). This finding demonstrates disruption of downstream mRNA secondary structure by a translationally coupled mRNA helicase activity while upstream sequences are being read.

Early studies of the path of mRNA through the ribosome correctly inferred that it wraps around the neck of the 30S subunit, entering through an opening between the head and shoulder and exiting behind the platform on the opposite side of the subunit (Frank et al., 1995; Shatsky et al., 1991). The path of mRNA was observed directly by X-ray crystallography, in Fourier difference maps, which showed the entry of the mRNA through the downstream tunnel between the neck and shoulder, the positioning of the A and P site codons on the interface surface of the 30S subunit, and passage through the upstream tunnel to the location of the Shine-Dalgarno helix in a pocket on the solvent side of the platform (Yusupova et al., 2001). Because the diameter of the downstream tunnel is too small to accommodate the dimensions of double-stranded RNA, it was concluded that any secondary structure in the translating mRNA must be disrupted either before entering the ribosome or at the entry to the tunnel itself.

It has not been possible thus far to identify the mRNA helicase since all of the relevant experiments have employed crude in vitro translation assays. To address this problem, we have developed a defined in vitro translation system using purified components that enables us to directly test the helix-unwinding ability of each of these components. Our assay monitors the displacement of RNA oligonucleotides base paired to downstream sequences of the mRNA during stepwise in vitro translocation. We find that a system containing purified *E. coli* ribosomes, mRNA, tRNAs, and elongation factors EF-Tu and EF-G is able to disrupt stably base-paired structures with melting temperatures of at least 70°C. Analysis of the register of the mRNA-oligonucleotide complexes in the ribosome places the helicase active site in the middle of the 30S downstream tunnel. Moreover, a reaction containing only ribosomes, aa-tRNAs, and the antibiotic sparsomycin can disrupt mRNA helices. These findings provide direct evidence that the mRNA helicase is the ribosome itself. Finally, mutation of arginines and lysines in proteins S3 and S4 that line the entry to the downstream tunnel confers loss of helicase activity, suggesting that the structure formed by proteins S3, S4, and S5, which encircle the incoming mRNA, plays a role in helicase processivity, similar to the sliding clamp of DNA replication (Kuriyan and O'Donnell, 1993).

Results

Throughout this paper, we use the mRNA numbering convention in which the A of the AUG (start) codon is defined as position +1 and downstream nucleotides are numbered accordingly. The "mRNA ribosomal register" is defined as the first nucleotide of the mRNA codon occupying the ribosomal P site; e.g. when the AUG codon occupies the ribosomal P site, the mRNA ribosomal register is +1.

Stepwise Translocation

We first developed a defined in vitro system to move the mRNA through the ribosome one codon at a time

*Correspondence: harry@nuvolari.ucsc.edu
[1]Present address: School of Medicine and Biomedical Sciences, Cary Hall, South Campus, The State University of New York at Buffalo, Buffalo, New York 14260.

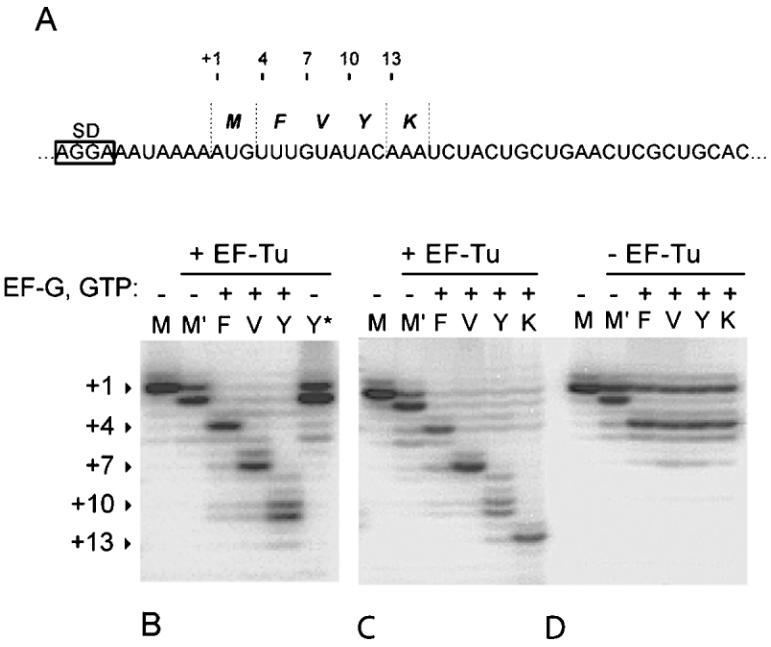

Figure 1. Toeprinting Analysis Showing Stepwise Translocation of m291 mRNA in a Defined In Vitro Translation System and Dependence on EF-G and EF-Tu

(A) The sequence of m291 mRNA and corresponding codons. The register of the mRNA (relative to +1 nucleotide, i.e., AUG) when each codon is positioned in the ribosomal P site is shown on the top. SD, Shine Dalgarno sequence.

(B) The register of the mRNA in the ribosomal P site is shown on the left. Lanes are labeled according to the tRNA species bound to the ribosomal P site at each step. M, N-Ac-Met-tRNA^{fMet} was bound to the mRNA-ribosome complex, followed by stepwise addition of M′, Phe-tRNA^{Phe}·EF-Tu·GTP; F, EFG and GTP; V, Val-tRNA^{Val}·EF-Tu·GTP; Y, Tyr-tRNA^{Tyr}·EF-Tu·GTP. Y*, similar to lane Y except that EF-G and GTP were absent.

(C) M, M′, F, V, and Y as in (B); K, addition of Lys-tRNA^{Lys}·EF-Tu·GTP.

(D) As for (C) but in the absence of EF-Tu.

in a controlled fashion. The AUG start codon of m291 mRNA (a gene 32 derivative) was positioned in the ribosomal P site by binding initiator tRNA (Figure 1A). Pure aminoacyl-tRNAs corresponding to the next four codons were introduced sequentially as aa-tRNA·EF-Tu·GTP ternary complexes, and coupled translocation of tRNA and mRNA was catalyzed by EF-G·GTP. Movement of the mRNA through the ribosome in one-codon steps was monitored by a primer extension (toeprinting) assay (Hartz et al., 1988; Joseph and Noller, 1998).

Figure 1 shows successive rounds of stepwise translocation of m291. Binding the initiator tRNA results in a strong toeprint band corresponding to positioning of the AUG start codon in the ribosomal P site (the +1 register; Figure 1B, lane M). Binding of Phe-tRNA^{Phe} ternary complex to the A site gives rise to a characteristic doublet band as observed previously (Fredrick and Noller, 2002; Joseph and Noller, 1998) (Figure 1B, lane M′); introduction of EF-G and GTP then causes translocation of mRNA by one codon (Figure 1B, lane F). In the same way, addition of the second, third, and fourth tRNA ternary complexes (Val-tRNA^{Val}, Tyr-tRNA^{Tyr}, and Lys-tRNA^{Lys}) corresponding to the next three successive codons results in stepwise translocation of mRNA into the +7, +10, and +13 ribosomal registers, respectively (Figures 1B and 1C, lanes V, Y, and K). Occasionally, the toeprint appeared as a doublet band, as seen after translocation of the Tyr codon into the P site (Figures 1B and 1C, lane Y).

Processive stepwise translocation under our experimental conditions is dependent on the presence of both elongation factors. When aminoacyl-tRNAs were introduced in the absence of EF-Tu, only partial translocation was observed in the first step (Figure 1D, lane F), and further translocations were barely detectable (Figure 1D, lanes V, Y, and K), consistent with the known importance of EF-Tu in binding tRNAs to the ribosomal A site (Pape et al., 1998). Conversely, in the absence of EF-G, no translocation was observed upon addition of ternary complexes (Figure1B, lane Y*).

Helicase Assay

We used an oligonucleotide displacement assay to monitor the ability of the ribosome to disrupt downstream secondary structure. A helix was formed in the path of the ribosome by annealing an end-labeled RNA reporter oligonucleotide to the mRNA, downstream from the ribosome binding region. Release of the bound oligonucleotide from the mRNA for each step of translocation was measured by gel electrophoresis under nondenaturing conditions.

First, we tested the helicase activity on a duplex formed at position +19 from a 12-nt oligomer paired to nucleotides +19 to +30 of m291 [H12(+19), Figure 2]. Free energy (ΔG_{37}) calculations (Nakano et al., 1999; Xia et al., 1998) predicted that this helix is stable under our experimental conditions (<10% oligo release), and that more than half of it will melt upon disruption of the first three base pairs at its upstream end; this was verified experimentally (data not shown; see Experimental Procedures).

Figure 3A shows the results of the helicase assay on the H12(+19)-m291 duplex, using the stepwise translocation described above (Figure 1). The free (single-stranded) and bound (double-stranded) forms of the end-labeled oligonucleotides at the end of each translocation step were resolved on a native gel. The H12(+19)-m291 helix remains stable after binding initiator tRNA and Phe-tRNA^{Phe} ternary complex and survives the first two translocation steps. Partial displacement (~25%) of the oligonucleotide is observed at the third translocation step (Figure 3A, lane Y), and release reaches ~85%–90% after the fourth step (Figure 3A, lane K).

When the translocation reaction was performed in the absence of EF-G or EF-Tu (as in Figure 1A, lane Y* or Figure 1C), no oligonucleotide was released (data not

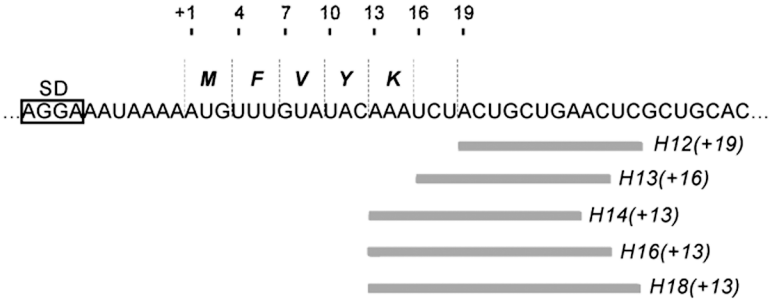

Figure 2. Oligonucleotides Used in the Helicase Assay

The sequence of m291 and the mRNA registers after each translocation step are shown as in Figure 1. Oligos are numbered according to their length and the position of their upstream end after base pairing with m291, e.g., H12 (+19) is a 12-mer that base pairs to nts +19 to +30.

shown). Furthermore, as noted above, even after two translocation steps, when all the components except Tyr-tRNA^{Tyr} and Lys-tRNA^{Lys} are present, no oligonucleotide displacement takes place (Figure 3A, lane V). None of the components used in this assay has any detectable helicase activity on its own. The observed helicase activity, therefore, must be the result of the translocation of mRNA through the ribosome.

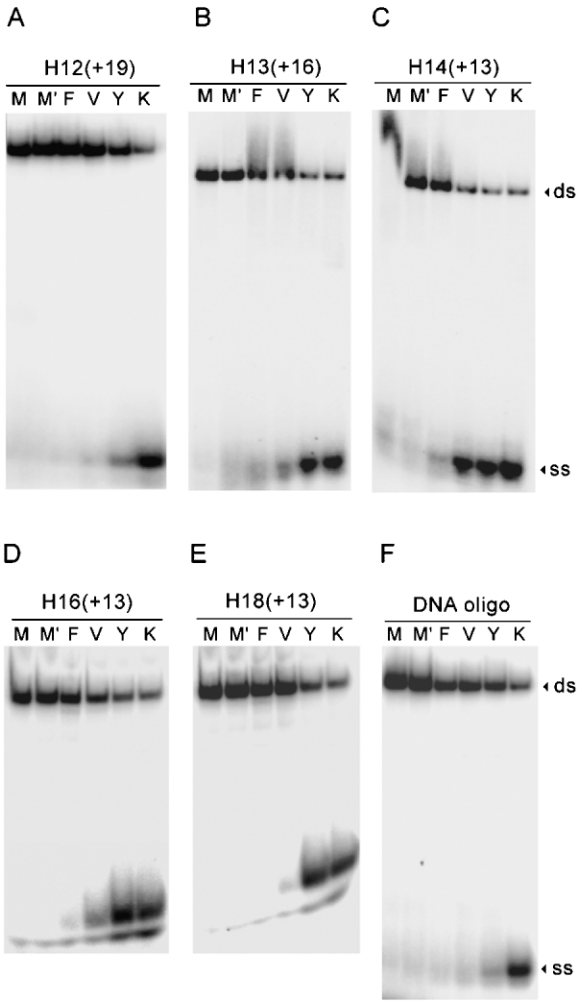

Figure 3. Helicase Assay Showing the Release Profiles of Various mRNA Bound RNA Oligos and One Reaction with a DNA Oligo

Oligos as shown in Figure 2. Lanes are labeled as in Figure 1, according to the tRNA species bound to the ribosomal P site at each step. ds, double-stranded; ss, single-stranded. Helicase assay with (A) H12(+19)-m291 duplex, (B) H13(+16)-m291 duplex, (C) H14(+13)-m291 duplex, (D) H16(+13)-m291 duplex, (E) H18(+13)-m291 duplex. (F) Same as (A) but with a DNA oligo.

We next performed helicase assays on duplexes formed at positions +16 and +13 of the mRNA with oligonucleotides H13(+16) and H14(+13) (Figure 2). The thermal stabilities of these helices were designed (and verified experimentally) to be similar to that of H12(+19). Dissociation of H13(+16) is detectable after two translocation steps (~30%) and reaches 80% after the third step (Figure 3B, lanes V and Y), whereas for H14(+13) these events occur after the first and second translocation steps, respectively (Figure 3C, lanes Y and K). Thus, as expected, when the helices were positioned 3 or 6 nucleotides closer to the ribosome, the oligos were released one or two translocation steps earlier.

In order to study the helicase activity on longer helices, a 16-mer [H16(+13)] or an 18-mer [H18(+13)] oligonucleotide were base paired to m291 at position +13 (Figure 2). Although the position of the upstream ends of these helices relative to the ribosome is identical to that of H14(+13), their higher calculated thermal stabilities predict that the bound oligos will dissociate only after disruption of the first seven and nine upstream base pairs. Figure 3D shows that for the H16(+13)-m291 duplex, 30% of the bound oligo is released after two translocation steps, approaching ~70%–80% after the third step (Figure 3E, lanes V and Y). In contrast, only 5% of the bound H18(+13) is displaced after the second translocation, but this reaches ~80% release after three translocations. These results show that, as predicted, the point of release of the oligos by the ribosome is dependent on duplex length (and hence thermal stability).

Helicase Activity on DNA/RNA Duplexes

When DNA oligonucleotides were used to form the helices at positions +13, +16, or +19, the oligonucleotides were released to the same extent and at the same step as observed for the corresponding RNA-RNA duplexes (Figure 3F; data not shown). The result of the helicase assay on the duplex formed from the H12(+19) DNA oligonucleotide is shown in Figure 3F. These experiments show that under our experimental conditions the ribosomal helicase does not distinguish between RNA-RNA and DNA-RNA duplexes and acts on both types of helices with comparable efficiency.

The Location of the Helicase Active Site

We used the findings from the helicase assay to estimate the location of the helicase active site, i.e., the point at

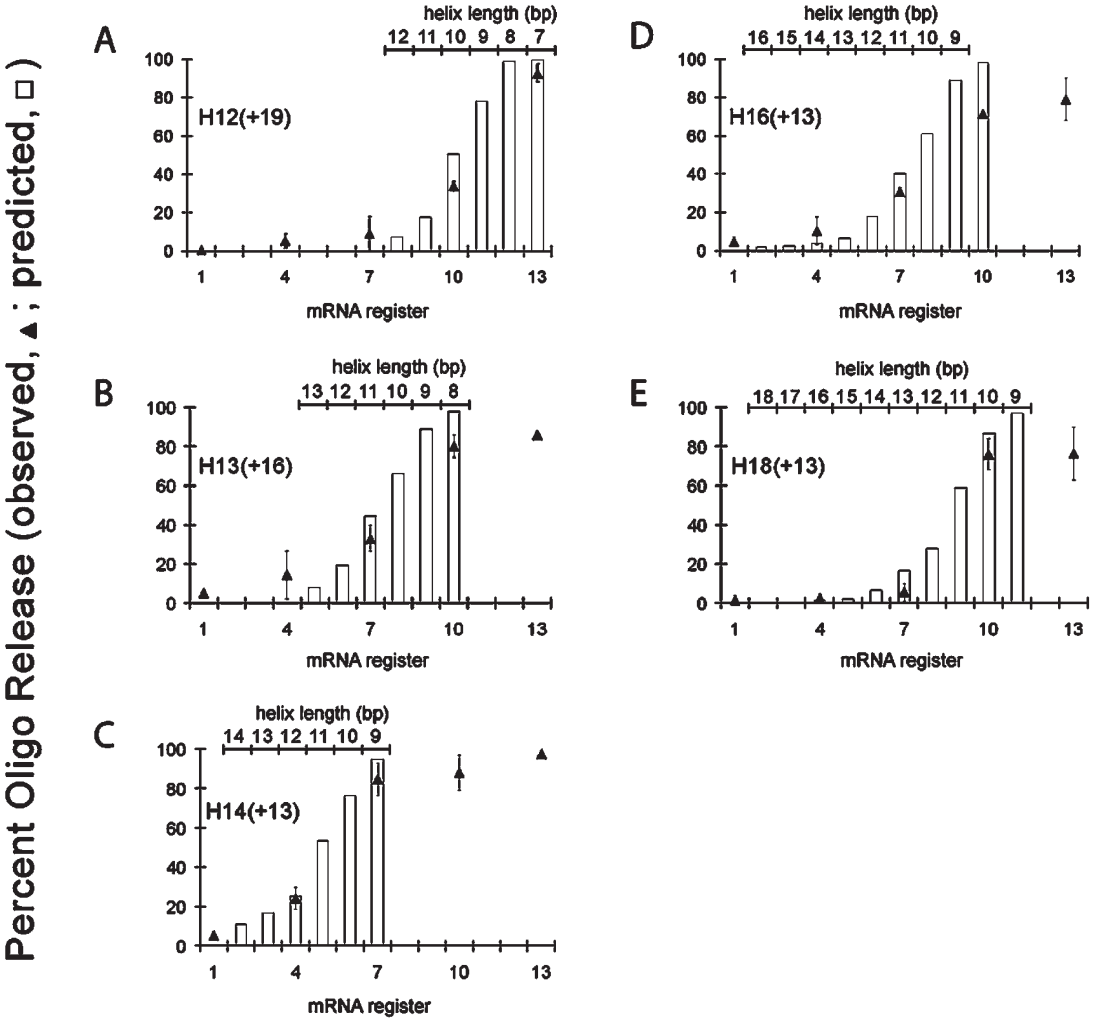

Figure 4. Fitting the Predicted and Observed Release Profiles

Triangles (▲) show the fraction of the oligo released (y axis) at each translocation step. The mRNA register (x axis) corresponds to the first nucleotide of the codon that occupies the ribosomal P site during that step. Error bars are from the results of three repetitions of each experiment. Histograms show the predicted release profile for each oligo, when the length of the corresponding helix (second x axis on top) is reduced by successive elimination of base pairs at its upstream end. The figure shows the agreement between the predicted and observed plots when the point of strand separation (upstream helix junction, see text) is placed 11 nt downstream from the P site.

which the two strands of an incoming helix are first separated. First, a predicted release profile was calculated for each oligo-mRNA helix. Based on the thermal stability of the remainder of the helix (Nakano et al., 1999; Xia et al., 1998), we calculated the percentage of bound oligo that will be released as the helix is sequentially disrupted (Figure 4, histograms; Experimental Procedures). The length of the helix in these histograms defines the position of the upstream helix junction. For example, when the length of the H12(+19)-m291 duplex is 12 base pairs (the full-length helix), the upstream helix junction is at +19, and when its length is reduced to 9 base pairs, the helix junction shifts from mRNA position +19 to +22 (corresponding to disruption of three upstream base pairs). Next, the theoretical profiles were fitted to the observed release profiles (the experimentally observed oligo release following each translocation) by sliding the theoretical plots along the x axis to achieve optimal correspondence between the two profiles. Finally, the location of the helicase active site was obtained by subtracting the position of the predicted upstream helix junction at each step from the ribosomal register of the mRNA at that step. For example, it was predicted that 95% of the bound H14(+13) will dissociate when the length of the duplex is decreased from 14 to 9 base pairs (by the disruption of five upstream base pairs between nucleotides +13 to +17 and the oligo), which shifts the upstream helix junction to +18 (Figure 4C, histogram). In the helicase assay this level of release was observed after two translocation steps (Figure 4C, triangles). Since the ribosomal register of the mRNA at this step is +7, the distance between the first nucleotide in the P site and the active site of the helicase on the mRNA is (18 − 7) = 11 nucleotides, i.e., the helicase disrupts the mRNA secondary structures at position +11. The same calculation was per-

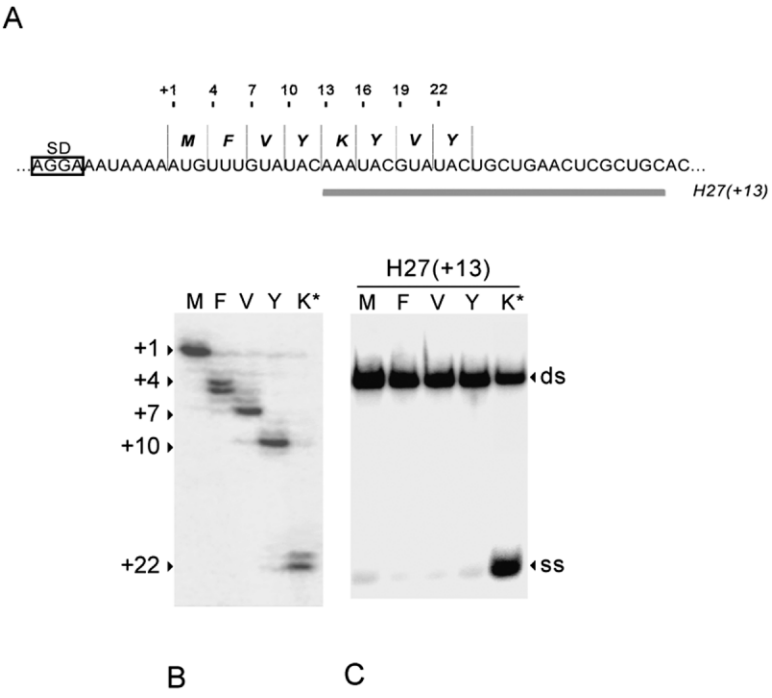

Figure 5. Helicase Assay on a 27-bp Helix

(A) The sequence of the mRNA after mutating the three codons downstream from Lys to "Tyr.Val.Tyr." H27(+13) base pairs with nts +13 to +39.

(B) Toeprint analysis of stepwise translocation with this mRNA. The register of the mRNA after each translocation step is shown on the left. M, N-Acetyl-Met- $tRNA^{fMet}$ was bound to the ribosomal P site followed by the addition of F, Phe-$tRNA^{Phe}$·EF-Tu·GTP and EFG and GTP; V, Val-$tRNA^{Val}$·EF-Tu·GTP; Y, Tyr-$tRNA^{Tyr}$·EF-Tu·GTP; K, Lys-$tRNA^{Lys}$·EF-Tu·GTP.

(C) Helicase assay on H27(+13)-mRNA duplex. The lanes correspond to those in (B).

formed for each data set yielding similar results. In all cases a close fit was obtained between the respective observed release profile and the theoretical profile (correlation coefficient ≈ 0.99). In some cases the data were also compatible with a 10-nt distance between the P site and the active site.

Processivity of the Ribosomal Helicase

As shown above (Figure 3E), the ribosome can disrupt nine successive base pairs and dissociate an 18-mer oligonucleotide from the mRNA. To further test the processivity of the helicase we formed a 27-base pair helix at position +13 (Figure 5A), whose calculated thermodynamic stability (T_m = 70.2) predicts release only after disruption of 18–20 base pairs. We mutated the m291 mRNA to allow translocation through eight codons to the +22 register (Figure 5B, lane K*). In the helicase assay, more than 65% of the bound oligo dissociates after eight rounds of translocation (Figure 5C, lane K*), showing that at least 18 base pairs were disrupted.

The Energy Source of the Ribosomal Helicase

Separation of the two strands of an RNA helix is an endergonic reaction, requiring an energy supply. Translocation of mRNA under our experimental conditions is EF-G and EF-Tu dependent (Figure 1). Both of these elongation factors are GTPases and are thus potential sources of energy for the helicase reaction.

Recently, it was shown that the low-molecular weight antibiotic sparsomycin can catalyze translocation in the absence of these factors and GTP (Fredrick and Noller, 2003). We therefore tested the helicase activity in a sparsomycin-dependent translocation reaction. Because sparsomycin remains tightly bound to the ribosome following translocation, it can catalyze only a single round. Therefore, it was necessary to create an oligo-mRNA duplex whose ribosomal register permits oligo release after translocation by a single codon. Accordingly, a duplex was formed at position +10 by binding H14(+10), complementary to nts +10 to +24 of m301. Deacylated $tRNA^{Tyr}$ was first bound to the UAC codon of m301 mRNA (Figure 6A) in the ribosomal P site (Figure 6B, lane Y); N-acetyl-Phe-$tRNA^{Phe}$, corresponding to the A site codon, was then added to the reaction, causing the appearance of the doublet toeprint band (Figure 6B, lane Y′). Similar to the case with EF-G (Figure 6B, lane F), addition of sparsomycin to this complex causes mRNA translocation by one codon (Figure 6B, lane F*). In the helicase assay, ~62% of the bound oligo was released after the addition of sparsomycin (Figure 6C, lane F*), compared to ~70% release with EF-G (Figure 6C, lane F), showing that the helicase can function even in the absence of GTP or added elongation factors.

Mutation of Basic Amino Acids Lining the Downstream Tunnel

Previously, we noted that proteins S3, S4, and S5 project basic amino acid side chains into the downstream tunnel from their positions surrounding the point of entry of the mRNA into the ribosome (Figure 7), which could make electrostatic contacts with phosphates in the mRNA backbone (Gavrilova and Spirin, 1971). Their close proximity to the predicted location of the helicase active site suggested that they might be involved in the mRNA helicase function. We tested this possibility by mutating them from Arg or Lys to Ala. For S3, we made the triple mutation R131A,R132A,K135A, for S4 the double mutation R44A,R47A, and for S5 the double mutation R19A,R28A. Mutant proteins were overexpressed, purified, and reconstituted into 30S subunits in vitro together with the other twenty wild-type proteins and 16S rRNA and tested for helicase and translocation activity after

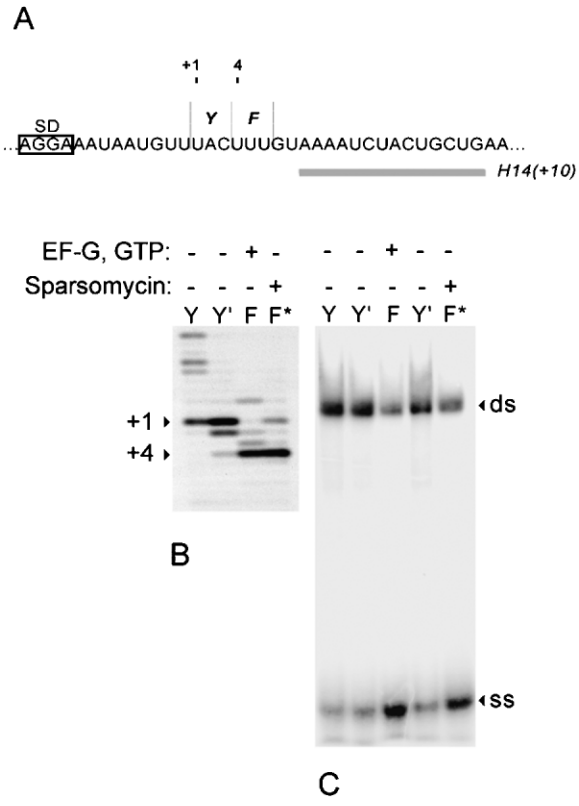

Figure 6. Comparison of Helicase Activity in Sparsomycin-Dependent Translocation with EF-G-Dependent Translocation

(A) The sequence of m301 mRNA. The first and second codon and the register of the mRNA when each of them is positioned in the ribosomal P site are shown on the top. H14(+10) binds to nts +10 to +23 of m301.

(B) Toeprint analysis on m301. Y, $tRNA^{Tyr}$ is bound to the ribosomal P site followed by the addition of Y′ N-Acetyl-Phe-$tRNA^{Phe}$; F, EF-G and GTP; or F*, sparsomycin.

(C) Helicase assay on H14(+10)-m301 duplex. Lanes are labeled as in (B).

association with 50S subunits, using the H27(+13) substrate. Ribosomes containing the different mutant proteins showed translocation efficiencies similar to that of wild-type (Figure 8A). The S5 double mutant had helicase activity comparable to that of wild-type, but the S3 and S4 mutants both showed deficiencies in the helicase assay (Figure 8B).

Discussion

To our knowledge, this is the first direct evidence that the ribosome itself has mRNA helicase activity. The use of a defined in vitro translation system, composed of purified ribosomes, mRNA, tRNAs, EF-G, and EF-Tu, shows that the basic translation machinery does not require exogenous factors, such as an ATP-dependent RNA helicase, to disrupt mRNA helices. Furthermore, none of the basic components has any detectable helicase activity on its own, indicating that the observed helix-unwinding activity must be the result of mRNA translocation. Controlled, stepwise translocation of mRNA made it possible to localize the site of helicase activity to the middle of the downstream tunnel of the 30S subunit, providing direct evidence that the helicase is the ribosome itself.

We tested the possible energetic contribution of the elongation factors to the helicase activity. The occurrence of translocation in the absence of EF-G or GTP has shown that translocation is most likely a thermodynamically spontaneous process, driven by differential affinities of the ribosomal binding sites for different tRNAs following peptide bond formation (Fredrick and Noller, 2003; Gavrilova and Spirin, 1971; Pestka, 1969; Southworth et al., 2002). Our observation that the ribosomal helicase also functions in the absence of EF-G, EF-Tu, GTP, or ATP (during sparsomycin-catalyzed translocation) indicates that the energy released during translocation is also sufficient to disrupt three base pairs of an mRNA duplex. Because of sparsomycin's inhibitory effect on translation, however, our observations on nonenzymatic translocation are limited to a single step, and the extent of helicase activity during rounds of successive nonenzymatic translocation remains unknown. Furthermore, since we have not measured the time course of these in vitro translocation reactions, the kinetic contributions of the elongation factors to the helicase activity, which may be of utmost importance in vivo, cannot be addressed.

Our data place the helicase active site at about position +11 of an mRNA bound to the ribosome in the +1 register. In the 70S crystal structure, this part of the mRNA is located inside the downstream tunnel, at a point where the average diameter of the tunnel is ~15 Å, somewhat smaller than that of an RNA helix. Interestingly, the predicted location of the helicase active site coincides with the optimal position for downstream pseudoknots that stimulate −1 frameshifting in many RNA viruses (Alam et al., 1999; Brierley et al., 1989; Brierley and Pennell, 2001). These pseudoknots are thought to cause ribosomes to pause while they are reading "shifty codons" at the junction of overlapping coding sequences, resulting in realignment of the ribosome in the −1 reading frame. Our results predict that frameshifting occurs when the downstream pseudoknot is positioned at the ribosomal helicase active site. A possible explanation is that a stereochemical mismatch between the structure of the pseudoknot and the helicase machinery in the downstream tunnel prevents unwinding of these structures, impeding forward motion of the mRNA.

What structural features does the helicase recognize? Since it must act on all mRNAs, the helicase activity must be sequence independent. Its ability to unwind RNA-DNA hybrid duplexes also indicates that its mechanism does not depend on recognition of the 2′-hydroxyl groups of the riboses. The other potential sites of recognition are the phosphate groups, which could interact with basic side chains of proteins S3, S4, and S5 that extend into the downstream tunnel, as suggested previously (Yusupova et al., 2001). Mutation of the basic side chains of S3 and S4 (but not S5) that protrude into the downstream tunnel causes significant loss of helicase activity, although the efficiency of EF-G-dependent translocation is unaffected in the mutant ribosomes (Figure 8). This suggests that electrostatic interactions between basic side chains of proteins S3 and S4 and

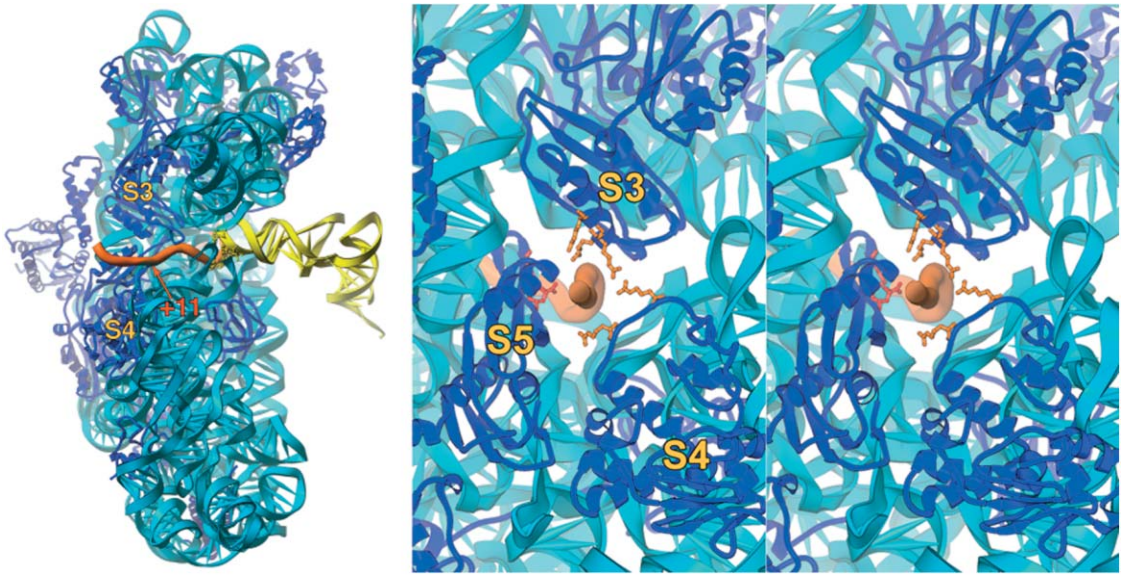

Figure 7. Position of mRNA in the Downstream Tunnel

(Left) Cross-section of the *T. thermophilus* 30S ribosomal subunit, showing the mRNA (orange), A site tRNA (yellow), and proteins S3 and S4. The +11 position of mRNA is indicated. (Right) View of the entry to the downstream tunnel, viewed from the solvent side, showing the mRNA surrounded by proteins S3, S4, and S5. The side chains mutated to alanine (R131, R132, and K135 in S3; R44 and R47 in S4; R19 and R28 in S5) are from the coordinates of the high-resolution *T. thermophilus* 30S subunit (Wimberly et al., 2000) and are shown in orange.

mRNA phosphate groups are important for helicase activity.

The ability of the ribosome to unwind a long, highly stable helix shows that it is a highly processive helicase, capable of successive disruption of many base pairs without dissociation from the mRNA. Processivity of DNA polymerases, which also depend on sequential disruption of a nucleic acid double helix, employs an annular protein complex termed the "sliding clamp" that surrounds the DNA during replication, preventing backsliding or dissociation of the DNA from the polymerase (Kuriyan and O'Donnell, 1993). Our findings are consistent with the possibility that proteins S3, S4, and S5, which form a ring around the incoming mRNA, act as a processivity clamp for the helicase function of ribosomes. Although mutation of Arg19 and Arg28 of S5 does not appear to have an effect on helicase activity, S5 may nevertheless play a role in enclosing the mRNA entry point by completing the ring of proteins at the mRNA entry point.

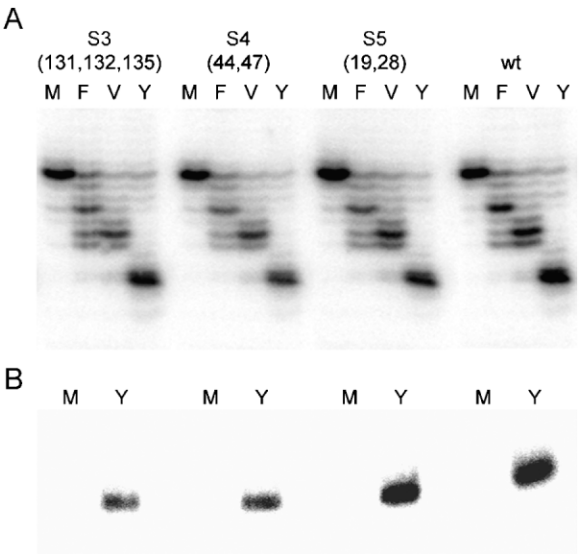

Figure 8. Effects of Mutations in S3, S4, and S5 on the Ribosomal Helicase Activity

Ribosomes containing mutations in S3 (R131A,R132A,K135A), S4 (R44A,R47A), or S5 (R19A, R28A) at basic side chains lining the downstream tunnel were assayed for (A) stepwise translocation and (B) helicase activity using the H27(+13) duplex.

It is believed that the mechanism of action of classical DNA and RNA helicases involves coupling the energy of hydrolysis of ATP to conformational changes in their protein structures (von Hippel and Delagoutte, 2001). But it is still a matter of debate whether they actively disrupt duplexes or take advantage of spontaneous fraying of the ends of helices to capture and stabilize their polynucleotide substrates in their single-stranded forms or whether both types of mechanism are used. No known helicase motifs are found among the ribosomal proteins, and no ATP is required for ribosomal helicase activity, suggesting that it is a novel type of helicase, possibly involving RNA as well as protein elements in its mechanism of action.

A shearing model for the ribosomal helicase was proposed previously (Yusupova et al., 2001), based on the observed rotational movement of the 30S head relative to the body during translocation (Agrawal et al., 1999). Since the site of action of the helicase is inside the downstream tunnel, at the interface between the head and the body of the 30S subunit, the opposing strands of an mRNA helix could bind to the head and body,

respectively. Movement of the head relative to the body would thus result in disruption of the helix. Our findings are also compatible with an alternative, passive model, analogous to the "inchworm" mechanism proposed for PcrA DNA helicase (Velankar et al., 1999; Yarranton and Gefter, 1979), in which spontaneous fraying, or breathing, of the terminal base pairs of a helix is followed by successive translocation of the mRNA and re-gripping of the mRNA by the putative S3-S4-S5 clamp.

The oligonucleotide displacement assay used to study the ribosomal helicase activity is not an exact mimic of the mRNA hairpin structures normally encountered by the ribosome during translation. Unlike our assay construct, neither of the strands of an mRNA hairpin entering the downstream tunnel has a free end, and hence the details of the interaction of real mRNA helices with the active site may differ. Future studies will need to address the properties of the ribosomal helicase using hairpins and other RNA structures.

Unwinding RNA or DNA helices is an essential step in many crucial physiological processes, including replication, DNA repair, recombination, transcription, pre-mRNA splicing, and translation (Delagoutte and von Hippel, 2003). In every case so far, unwinding has been found to be carried out by separate, dedicated helicase proteins. In translation, however, helicase activity is embodied in the ribosome itself. The "power stroke" of the ribosomal helicase appears to be provided by translocation, a reaction normally driven by GTP hydrolysis catalyzed by elongation factor EF-G. However, spontaneous translocation has been shown to occur under certain in vitro conditions (Gavrilova and Spirin, 1971; Pestka, 1969; Southworth et al., 2002), such as sparsomycin-induced translocation (Fredrick and Noller, 2003), driven presumably by the differential binding affinities of the aminoacyl-, peptidyl-, and deacylated tRNAs to their respective ribosomal binding sites. The ability of the ribosomal helicase to act in the absence of elongation factors EF-G and GTP suggests that it is driven, or can be driven, by the same differential binding energies. The inescapable presence of secondary structure within mRNA coding sequences must have been one of the first problems encountered in the transition from an RNA world to a protein world and may have resulted in coupling of ribosomal helicase activity with the fundamental mechanics of translocation. In their studies of ratcheting of the two ribosomal subunits between the pre- and posttranslocation states, Frank and Agrawal (2000) observed a reciprocal expansion and contraction in the diameter of the upstream and downstream tunnels, suggesting that these two features may alternately grab and release the mRNA during translocation of mRNA. This dynamic behavior in the downstream tunnel could also be related to its helicase function.

Experimental Procedures

mRNAs

m291 mRNA was transcribed by T7 RNA polymerase from linearized PKF291 plasmid (Fredrick and Noller, 2002) and purified on a 6% denaturing polyacrylamide gel. To allow eight-codon translocation, three codons downstream from the Lys codon (Ser.Thr.Ala, TCTACTGCT) in the open reading frame of PKF291 were mutated to Tyr.Val.Tyr (TACGTATAC) by site-directed mutagenesis (Quikchange, Stratagene); an mRNA was transcribed from this plasmid and purified as described above. m301 mRNA was a gift from K. Fredrick.

Oligonucleotides

RNA oligonucleotides H12(+19) (GAGUUCAGCAGU), H13(+16) (GUUCAGCAGUAGA), H14(+13) (UCAGCAGUAGAUUU), H16(+13) (GUUCAGCAGUAGAUUU), H18(+13) (GAGUUCAGCAGUAGAUUU), and H27(+13) (GCAGCGAGUUCAGCAGUAUACGUAUUU) were synthesized by Dharmacon and purified on a 12% denaturing polyacrylamide gel. H14(+10) that was used in the helicase assay with m301 has the same sequence as H14(+13) above. DNA oligonucleotides with sequences corresponding to the six RNA oligonucleotides above, and AL2 toeprinting primer (TCTTCAGAAAGAAAAACC), were synthesized by Fisher Oligos and purified on a 12% denaturing polyacrylamide gel.

Thermodynamic Calculations

Thermodynamic stabilities of the mRNA-oligo duplexes (free energies of the duplexes at 37°C; ΔG_{37}) were calculated according to the nearest neighbor method with corrections for NH_4Cl and $Mg(OAc)_2$ concentrations in the helicase assay (Nakano et al., 1999; Xia et al., 1998). The release profiles of the oligo-mRNA duplexes were derived from the calculated free energies (ΔG_{37}) for different lengths of each duplex:

$$K = \exp[-\Delta G_{37}(T)/RT] = \alpha/[(mRNA_T - \alpha\ oligo_T)(1 - \alpha)]$$

Where K is the equilibrium constant, T is the temperature in deg Kelvin, R is the gas constant (1.987cal deg^{-1} mol^{-1}), α is the fraction of oligos in duplex form, and $mRNA_T$ and $oligo_T$ are the total concentrations of the mRNA and the oligo in the reaction, respectively.

Duplex Stability Assay

H12(+19), H13(+16), and H14(+13) and their n-3 counterparts [H9(+22), H10(+19), and H11(+10), respectively] were tested in a duplex stability assay, under conditions similar to the helicase assay (below). One picamole of each [^{32}P]-labeled oligonucleotide was first annealed to 1.5 pmol mRNA in 10 μl of 10 mM Tris-HCl (pH 7.4) and 60 mM NH_4Cl, by heating to 90°C for 1 min, incubation at 60°C for 5 min, addition of $MgCl_2$ (10 mM), and cooling to room temperature over 10 min. Binding buffer [10 mM Tris-HCl (pH 7.4), 60 mM NH_4Cl, 10 mM $Mg(OAc)_2$, 6 mM β-ME] was then added to a final volume of 30 μl, and the reaction incubated for 1 hr at 37°C . A 2 μl aliquot of this reaction was quenched on ice by the addition of 2 μl 5× loading buffer (50% glycerol, 2% SDS, 20 mM EDTA, and 0.01% bromophenol blue and xylene cyanol) and 6 μl distilled water, loaded on a running 6% nondenaturing polyacrylamide gel at 4°C, and electrophoresed for 1 hr. Gels were dried and quantified using a Molecular Dynamics Phosphorimager.

tRNAs and Elongation Factors

Purified tRNAs were purchased from Subriden ($tRNA^{fMet}$, $tRNA^{Val1}$, $tRNA^{Tyr2}$) or Sigma ($tRNA^{Lys}$, $tRNA^{Phe}$) and aminoacylated using DEAE-purified S100 enzymes as previously described (Moazed and Noller, 1989). Aminoacylated tRNAs were purified from the charging reaction and the efficiency of aminoacylation in each case was checked by acid gel electrophoresis (Fredrick and Noller, 2002). EF-G was purified and stored as previously described (Fredrick and Noller, 2002). A C-terminal histidine-tagged EF-Tu was overexpresssed in *E. coli* BL21 (DE3) and purified from the soluble extract on an Ni^{2+}-agarose column as previously described (Boon et al., 1992), with minor modifications.

Ternary Complexes

EF-Tu·GDP (~300 pmol) was incubated with GTP (1 mM), phosphoenol pyruvate (3 mM), and pyruvate kinase (100 μg/ml) in 20 μl of 50 mM Tris·HCl (pH 7.5), 40 mM NH_4Cl, 10 mM $MgCl_2$, and 1 mM DTT for 10 min at 37°C to exchange the bound GDP with GTP and then added to equimolar amounts of aminoacylated tRNA in the same buffer and further incubated for 5 min at the same temperature. Ternary complexes thus formed were added to the stepwise translocation reaction (below).

Stepwise Translocation

Tight-couple 70S ribosomes (1 μM final concentration) from *E. coli* MRE600 (Moazed and Noller, 1989) were incubated with m291 mRNA (50 nM) in 30 μl binding buffer (10 mM Tris·HCl [pH 7.4], 60 mM NH_4Cl, 10 mM $Mg(OAc)_2$, 6 mM β-ME) for 10 min at 37°C, followed by addition of N-Acetyl-Met-$tRNA^{fMet}$ to 1 μM and a further 10 min incubation to fill the P site. Aliquots (5 μl) of this reaction were then added to separate tubes containing either GTP (600 μM) (M), GTP + Phe-$tRNA^{Phe}$ ternary complex (1 μM) (M′), GTP + Phe-$tRNA^{Phe}$ ternary complex + EF-G (2 μM) (F), GTP + Phe-$tRNA^{Phe}$ ternary complex + EF-G + Val-$tRNA^{Val}$ ternary complex (1 μM) (V), GTP + Phe-$tRNA^{Phe}$ ternary complex + EF-G + Val-$tRNA^{Val}$ ternary complex + Tyr-$tRNA^{Tyr}$ ternary complex (1 μM) (Y), or GTP + Phe-$tRNA^{Phe}$ ternary complex + EF-G + Val-$tRNA^{Val}$ ternary complex + Tyr-$tRNA^{Tyr}$ ternary complex + Lys-$tRNA^{Lys}$ ternary complex (1 μM) (K), in binding buffer (final volume, 10 μl). These tubes were incubated for 10 min at 37°C and then placed on ice for the next step (primer extension in toeprinting analysis or loading on a native gel in the helicase assay).

Toeprinting Assay

In the toeprinting assay, 1.5 pmole of m291 mRNA was first annealed to 2 pmole of [^{32}P]-labeled AL2 primer in 10 mM Tris·HCl (pH 7.4), 60 mM NH_4Cl by heating to 60°C for 3 min and placing on ice, followed by the addition of $MgCl_2$ (10 mM), prior to its addition to the stepwise translocation reaction (above). After translocation, aliquots (5 μl) of the reactions (M, M′, F, V, Y, and K) were extended in the binding buffer (10 μl final volume) containing 1 unit of AMV reverse transcriptase (Seikagaku America) and the four dNTPs (375 μM each) at 37°C for 10 min and the products resolved on a 6% sequencing gel (Fredrick and Noller, 2002; Joseph and Noller, 1998).

Helicase Assay

Duplexes were formed by annealing the mRNA and end-labeled oligos as described for the duplex stability assay. These duplexes were then used in the stepwise translocation reaction (above). After translocation, 2 μl aliquots of each reaction (tubes M, M′, F, V, Y, and K) were quenched on ice by the addition of 2 μl 5× loading buffer (50% glycerol, 2% SDS, 20 mM EDTA, and 0.01% bromophenol blue and xylene cyanol) and 6 μl distilled water to a final volume of 10 μl, loaded on a running 6% nondenaturing polyacrylamide gel, and electrophoresed at 4°C for 1 hr. Gels were dried and quantified using a Molecular Dynamics Phosphorimager. Oligonucleotide displacement was determined by measuring the amounts of end-labeled oligos in single-stranded (ss) and double-stranded (ds) forms and expressed as ss/(ss + ds).

Fitting of the theoretical and observed release profiles was performed as described in the text, by sliding the theoretical plot along the x axis to achieve maximal overlap between the two plots. The extent of fitting was tested by calculating the correlation coefficient.

Construction of Mutant Ribosomes

Mutation of residues R131, R132, and K135 in S3, R44 and R47 in S4, and R19 and R28 in S5 to alanines was done by changing the respective arginine or lysine codons to GCU alanine codons using the method of Kunkel (Kunkel, 1985) and verified by DNA sequencing. Mutant ribosomal proteins were individually overexpressed, purified by FPLC, and reconstituted in vitro with the other 20 wild-type proteins and 16S rRNA into 30S subunits on a 300 pmol scale essentially as described (Culver and Noller, 1999). Reconstituted mutant and wild-type 30S subunits were isolated by sucrose gradient centrifugation, combined with wild-type, natural 50S subunits, and assayed for their translocation and mRNA helicase activities as described above.

Acknowledgments

This work was supported by grant GM-17129 from the NIH, grant no. MCB-02112689 from the NSF, and a grant to the Center for Molecular Biology of RNA from the W.M. Keck Foundation. R.P.H. was supported by an Else Adler Postdoctoral Fellowship from the Damon Runyon Cancer Research Foundation. We thank K. Lieberman, K. Fredrick, and L. Lancaster for helpful discussions and for supplying materials. We are grateful to E. Dratz and A. Rich for discussions concerning their early unpublished mRNA helicase studies.

Received: August 13, 2004
Revised: October 15, 2004
Accepted: November 19, 2004
Published: January 13, 2005

References

Agrawal, R.K., Heagle, A.B., Penczek, P., Grassucci, R.A., and Frank, J. (1999). EF-G-dependent GTP hydrolysis induces translocation accompanied by large conformational changes in the 70S ribosome. Nat. Struct. Biol. *6*, 643–647.

Alam, S.L., Atkins, J.F., and Gesteland, R.F. (1999). Programmed ribosomal frameshifting: much ado about knotting! Proc. Natl. Acad. Sci. USA *96*, 14177–14179.

Boon, K., Vijgenboom, E., Madsen, L.V., Talens, A., Kraal, B., and Bosch, L. (1992). Isolation and functional analysis of histidine-tagged elongation factor Tu. Eur. J. Biochem. *210*, 177–183.

Brierley, I., Digard, P., and Inglis, S.C. (1989). Characterization of an efficient coronavirus ribosomal frameshifting signal: requirement for an RNA pseudoknot. Cell *57*, 537–547.

Brierley, I., and Pennell, S. (2001). Structure and function of the stimulatory RNAs involved in programmed eukaryotic-1 ribosomal frameshifting. In Cold Spring Harbor Symposia on Quantitative Biology: The Ribosome (Cold Spring Harbor, New York: Cold Spring Harbor Laboratory Press), pp. 233–248.

Culver, G.M., and Noller, H.F. (1999). Efficient reconstitution of functional Escherichia coli 30S ribosomal subunits from a complete set of recombinant small subunit ribosomal proteins. RNA *5*, 832–843.

Delagoutte, E., and von Hippel, P.H. (2003). Helicase mechanisms and the coupling of helicases within macromolecular machines. Part II: Integration of helicases into cellular processes. Q. Rev. Biophys. *36*, 1–69.

Doty, P., Boedtker, H., Fresco, J.R., Haselkorn, R., and Litt, M. (1959). Secondary structure in ribonucleic acids. Proc. Natl. Acad. Sci. USA *45*, 482–499.

Favre, A., Morel, C., and Scherrer, K. (1975). The secondary structure and poly(A) content of globin messenger RNA as a pure RNA and in polyribosome-derived ribonucleoprotein complexes. Eur. J. Biochem. *57*, 147–157.

Frank, J., and Agrawal, R.K. (2000). A ratchet-like inter-subunit reorganization of the ribosome during translocation. Nature *406*, 318–322.

Frank, J., Zhu, J., Penczek, P., Li, Y., Srivastava, S., Verschoor, A., Radermacher, M., Grassucci, R., Lata, K.R., and Agrawal, R.K. (1995). A model of protein synthesis based on cryo-electron microscopy of the *E. coli* ribosome. Nature *376*, 441–444.

Fredrick, K., and Noller, H.F. (2002). Accurate translocation of mRNA by the ribosome requires a peptidyl group or its analog on the tRNA moving into the 30S P site. Mol. Cell *9*, 1125–1131.

Fredrick, K., and Noller, H.F. (2003). Catalysis of ribosomal translocation by sparsomycin. Science *300*, 1159–1162.

Gavrilova, L.P., and Spirin, A.S. (1971). Stimulation of "non-enzymic" translocation in ribosomes by p-chloromercuribenzoate. FEBS Lett. *17*, 324–326.

Hartz, D., McPheeters, D.S., Traut, R., and Gold, L. (1988). Extension inhibition analysis of translation initiation complexes. Methods Enzymol. *164*, 419–425.

Holder, J.W., and Lingrel, J.B. (1975). Determination of secondary structure in rabbit globin messenger RNA by thermal denaturation. Biochemistry *14*, 4209–4215.

Joseph, S., and Noller, H.F. (1998). EF-G-catalyzed translocation of anticodon stem-loop analogs of transfer RNA in the ribosome. EMBO J. *17*, 3478–3483.

Kunkel, T.A. (1985). Rapid and efficient site-specific mutagenesis without phenotypic selection. Proc. Natl. Acad. Sci. USA *82*, 488–492.

Kuriyan, J., and O'Donnell, M. (1993). Sliding clamps of DNA polymerases. J. Mol. Biol. *234*, 915–925.

Lingelbach, K., and Dobberstein, B. (1988). An extended RNA/RNA duplex structure within the coding region of mRNA does not block translational elongation. Nucleic Acids Res. *16*, 3405–3414.

Min Jou, W., Haegeman, G., Ysebaert, M., and Fiers, W. (1972). Nucleotide sequence of the gene coding for the bacteriophage MS2 coat protein. Nature *237*, 82–88.

Moazed, D., and Noller, H.F. (1989). Interaction of tRNA with 23S rRNA in the ribosomal A, P, and E sites. Cell *57*, 585–597.

Nakano, S., Fujimoto, M., Hara, H., and Sugimoto, N. (1999). Nucleic acid duplex stability: influence of base composition on cation effects. Nucleic Acids Res. *27*, 2957–2965.

Pape, T., Wintermeyer, W., and Rodnina, M. (1998). Complete kinetic mechanism of elongation factor Tu-dependent binding of aminoacyl-tRNA to the A site of the E. coli ribosome. EMBO J. *17*, 7490–7497.

Pestka, S. (1969). Studies on the formation of transfer ribonucleic acid-ribosome complexes. VI. Oligopeptide synthesis and translocation on ribosomes in the presence and absence of soluble transfer factors. J. Biol. Chem. *244*, 1533–1539.

Shatsky, I.N., Bakin, A.V., Bogdanov, A.A., and Vasiliev, V.D. (1991). How does the mRNA pass through the ribosome? Biochimie *73*, 937–945.

Southworth, D.R., Brunelle, J.L., and Green, R. (2002). EFG-independent translocation of the mRNA:tRNA complex is promoted by modification of the ribosome with thiol-specific reagents. J. Mol. Biol. *324*, 611–623.

van Himbergen, J., van Geffen, B., and van Duin, J. (1993). Translational control by a long range RNA-RNA interaction; a basepair substitution analysis. Nucleic Acids Res. *21*, 1713–1717.

Velankar, S.S., Soultanas, P., Dillingham, M.S., Subramanya, H.S., and Wigley, D.B. (1999). Crystal structures of complexes of PcrA DNA helicase with a DNA substrate indicate an inchworm mechanism. Cell *97*, 75–84.

von Hippel, P.H., and Delagoutte, E. (2001). A general model for nucleic acid helicases and their "coupling" within macromolecular machines. Cell *104*, 177–190.

Wimberly, B.T., Brodersen, D.E., Clemons, W.M., Jr., Morgan-Warren, R.J., Carter, A.P., Vonrhein, C., Hartsch, T., and Ramakrishnan, V. (2000). Structure of the 30S ribosomal subunit. Nature *407*, 327–339.

Xia, T., SantaLucia, J., Jr., Burkard, M.E., Kierzek, R., Schroeder, S.J., Jiao, X., Cox, C., and Turner, D.H. (1998). Thermodynamic parameters for an expanded nearest-neighbor model for formation of RNA duplexes with Watson-Crick base pairs. Biochemistry *37*, 14719–14735.

Yarranton, G.T., and Gefter, M.L. (1979). Enzyme-catalyzed DNA unwinding: studies on Escherichia coli rep protein. Proc. Natl. Acad. Sci. USA *76*, 1658–1662.

Yusupova, G.Z., Yusupov, M., Cate, J.H.D., and Noller, H.F. (2001). The path of messenger RNA through the ribosome. Cell *106*, 233–241.